Anomalous absorption of 1-μm laser radiation by laser-produced plasmas

Andrew Perry, Barry Luther-Davies, and Ranko Dragila
Laser Physics Centre, The Research School of Physical Sciences, The Australian National University, P.O. Box 4, Canberra, Australian Capital Territory 2601, Australia
(Received 20 June 1988)

We present the results of experiments where we have measured the absorption of laser light by plasmas generated by 20–120-psec duration pulses of Nd laser radiation incident upon solid targets at intensities exceeding 10^{14} W/cm^2. The results were obtained using box calorimetry, supported by ion calorimetry, ion probe data, and 2ω calorimetry. We have found a marked asymmetry in the absorption for 120-psec pulses with irradiation geometry with the absorption dropping by 60% when the beam diverged at the target surface. The results were analyzed using a simple rigid plasma model and show that resonance absorption is not the dominant mechanism, but the absorption is caused by the presence of a narrow region near the critical surface having a strongly enhanced collision frequency most probably due to the presence of long-wavelength ion acoustic waves in the plasma.

INTRODUCTION

An understanding of the mechanisms by which intense laser radiation is absorbed by a plasma is fundamental to the process of laser-driven inertial confinement fusion and particularly in the late 1970s and early 1980s much experimental research was undertaken to elucidate the various absorption mechanisms.[1–5] Broadly speaking, the results were interpreted as showing that long-pulse, short-wavelength (visible and uv) radiation at moderate intensities ($I\lambda^2 \approx 10^{14}$ W μm^2/cm^2) was absorbed mainly by the classical inverse Bremsstrahlung process, while for short pulses of long-wavelength (infrared) light at moderate to high intensities ($I\lambda^2 \approx 10^{14}$–$10^{16}$ W μm^2/cm^2) resonance absorption dominated.[6–8] In the case of long-wavelength radiation it was frequently necessary, however, in explaining the experimental data to invoke a role for anomalous processes (ion acoustic turbulence, magnetic fields, critical surface rippling or curvature, the parametric decay instability, etc.). The first evidence that these anomalous mechanisms could in fact dominate the absorption came from the results of measurements using very high intensity ($I\lambda^2 \approx 10^{18}$ W μm^2/cm^2) CO_2 laser radiation where a rapid increase in absorption with increasing intensity was reported[9] near 10^{16} W/cm^2. Since the Nd:glass laser available at the Australian National University (ANU) is capable of operating at similar values of $I\lambda^2$ the original motivation for this work was to investigate whether an increase in absorption was also observed for 1-μm radiation in similar conditions. No significant rise in absorption was obtained, however, in a very careful study where absorption was deduced using an accurate box calorimeter, the absorption was found to be sensitive to the irradiation geometry in a way that was inconsistent with the widely held belief that resonance absorption was the most important mechanism. In fact the results could only be explained by invoking a dominant role for one of the anomalous processes for intensities even as low as $I\lambda^2 \approx 10^{14}$ Wμm^2/cm^2. Although our results could not unequivocally determine which mechanism was operating, the data were consistent with the view that long-wavelength ion-acoustic turbulence was causing a strong localized increase in the effective collision frequency in a narrow region near the critical density surface. More than 60% of the total absorption occurred in this region with the remaining 40% attributable to classical inverse bremsstrahlung and resonance absorption.

EXPERIMENTAL DATA

The experimental apparatus was as follows. The output beam from the ANU high brightness Nd:glass laser was focused onto planar glass targets using an $F=1$ aspheric focusing lens. The laser produced a few joules of energy in pulses whose duration could be selected between 20, 80, and 120 psec. The shortest pulses were generated using an active-passive mode-locked oscillator while for the longer ones a sophisticated actively mode-locked actively Q-switched system was available. The targets themselves were made from portions of glass microscope cover slips ensuring that the initial surface was smooth and flat and could be aligned very accurately (to within ± 5 μm) with respect to the focus of the lens. The choice of glass targets also minimized the errors introduced into the measurements by the buildup of target debris in the box calorimeter. The spot distribution near the focus of the lens was determined by reimaging the attenuated beam onto infrared sensitive film via a multiple image camera using a flat field microscope objective. The resulting images were digitized using a Perkin-Elmer scanning microdensitometer and corrected for the film response allowing conversion to local laser intensity. In best focus the focal spot had a FWHM of 3.8 μm with 90% of the incident energy contained within a diameter of 9.4 μm. Using the shortest pulses available for these experiments (20 psec) this corresponded to a peak in vacuum intensity of 2×10^{18} W/cm^2. Out of the focal plane

the beam developed ring structures with intensity excursions of typically a factor of 4. Although some variation in the details of the intensity patterns existed between equivalent positions either side of the focal plane, on a radially averaged basis these were small.

Absorption was determined using a box calorimeter based on the design of Gunn and Rupert[10] but with an improved calibration system and increased sensitivity of 3 mV/J to facilitate measurements with the low available laser energy. Incident, backscattered and transmitted light calorimeters were also employed so that radiation was collected over 92% of the total solid angle surrounding the target. The main regions of loss were at the corners of the box calorimeter and through the various apertures needed for target mounting and viewing. By careful cross calibration of the detectors and extrapolation to correct for the remaining losses from the system the overall uncertainty in the absorption did not exceed 5%. In addition to the box calorimeter measurements, absorption data was also collected from an ion calorimeter array, also similar to those described by Gunn and Rupert, and Faraday cup ion probes. Measurements were also made of the total amount of absorbed energy transferred into superthermal electrons penetrating the target; the superthermal electrons energy distribution function; and the total conversion of laser energy to its second harmonic. These last measurements were made by surrounding the target by a parabolic reflector which directed the 2ω emission to a calorimeter filtered with BG18 glass. The 2ω light emitted back through the focusing lens was also measured. Spectral measurements confirmed that second harmonic emission from the plasma dominated the radiation collected by these calorimeters.

Since only limited laser energy was available, the laser intensity was changed by holding the laser power constant and moving the target surface relative to the focal plane of the lens. Movements were made both towards (positive defocus) and away (negative defocus) from the lens for pulse durations of either 20 or 120 psec. This simple experiment revealed a most intriguing result shown in Figs. 1(a) and 1(b). For the 20-psec duration pulses the absorption fluctuated between 20% and 40% as the target was tracked through the focus with the highest absorptions obtained near best focus (at the highest intensity) and also at the largest defocus (lowest intensity). The minimum absorption occurred with the target 50 μm behind the focus where there is some evidence of a weak dip not apparent when the target is located the same distance in front of the focal plane. Overall, however, these data are in excellent agreement with previous data on absorption when plotted as a function of intensity (Fig. 2). It shows that the absorption increases with decreasing intensity below about 4×10^{14} W/cm^2 reflecting a rise in inverse Bremsstrahlung absorption due to the cooler plasmas produced at low intensity, and a slight increase in absorption with intensity above 4×10^{14} W/cm^2 which is normally taken to indicate increasing efficiency of resonance absorption because of profile modification. The weak apparent dip in absorption at -50 μm does not seriously disturb this picture.

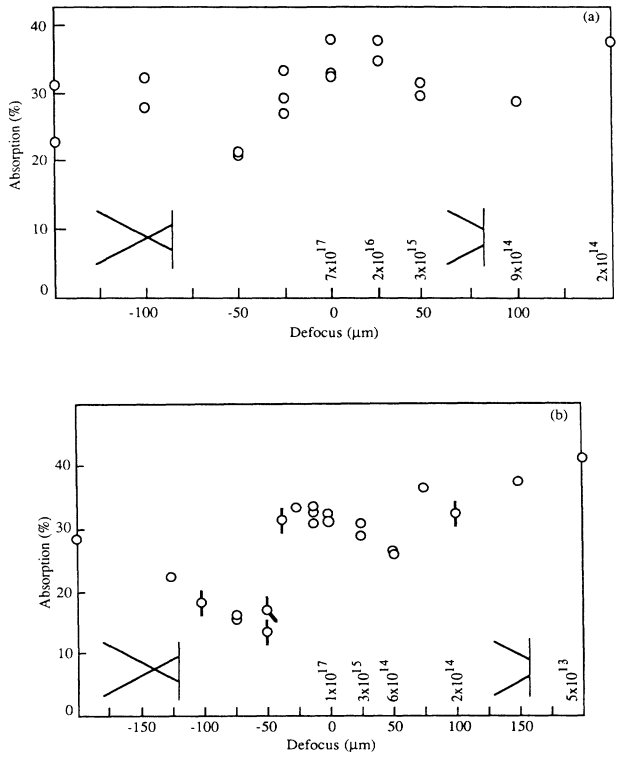

FIG. 1. Absorption as a function of target position: (a) 20-psec pulse; (b) 120-psec pulse.

For 120-psec duration pulses, however, the variation of absorption with target position shows a much more dramatic behavior. For positive defocus (target moved towards the lens) the absorption is similar to that for the 20-psec pulses and as a function of intensity the data fit neatly on Fig. 2. However, for negative defocus (target moved away from the lens) there is a sudden drop in absorption at about -37 μm from 35% to 15% and a markedly lower total absorption at all subsequent posi-

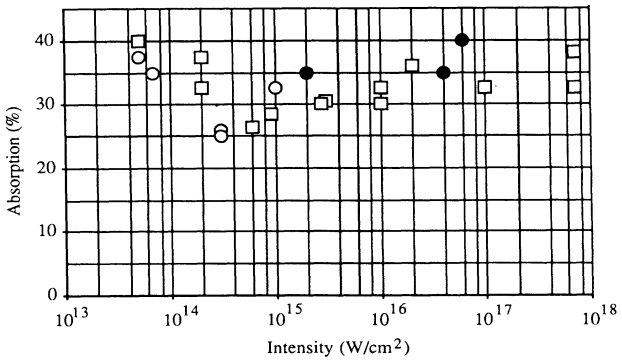

FIG. 2. Absorption for positive defocus (20- and 120-psec pulses) plotted as a function of intensity. Included for comparison are results from: ●, Haas *et al.* (Ref. 1) and ○, Garban-Labaune *et al.* (Ref. 7).

tions out to the measurement limit of -200 μm. This drop in absorption corresponds to the same weak feature observed for the 20-psec pulse case however, here the effect is very much enhanced.

Additional insight into the nature of the drop in absorption at -37 μm can be obtained by replotting the data to show the variation in the energy detected in the box and backscatter calorimeters as a function of the target position. This is shown in Figs. 3(a) and 3(b). In the case of the 120-psec duration pulses a large change in the distribution of the scattered light is apparent at the point where the absorption drops. Specifically near the minimum absorption the radiation scattered back through the focusing lens drops almost to zero while at the same time that received by the box calorimeter climbs to nearly 80%. The effect is nowhere near as apparent for 20-psec duration pulses. The 120-psec data suggest a strong role for geometry. Clearly a major difference between positive and negative defocus is that in the former case the radiation converges on the target and in the latter it diverges. If the isodensity contours were planar, as might be expected for the shortest duration pulses, then such a change in beam geometry would have little effect on the distribution of the scattered light. This fits the case for the 20-psec pulses. For longer pulses, however, the isodensity contours become convex because the plasma expansion is no longer one dimensional, and the change from a converging to diverging beam would result in a completely different range of angles of incidence within the plasma. This would lead to the observed scattered light behavior for the 120-psec duration pulses because for negative focal positions the radiation strikes the plasma at large angles of incidence and hence would be refracted sideways into the box calorimeter while for an equivalent positive defocus, the radiation strikes the plasma at closer to normal incidence. We can, therefore, conclude that the drop in absorption at -37 μm is simply telling us that the absorption is low for rays striking the plasma at non-normal incidence. This geometrical dependence immediately raises questions as to whether the data are consistent with a high level of resonance absorption which would be expected to favor the non-normal rays.

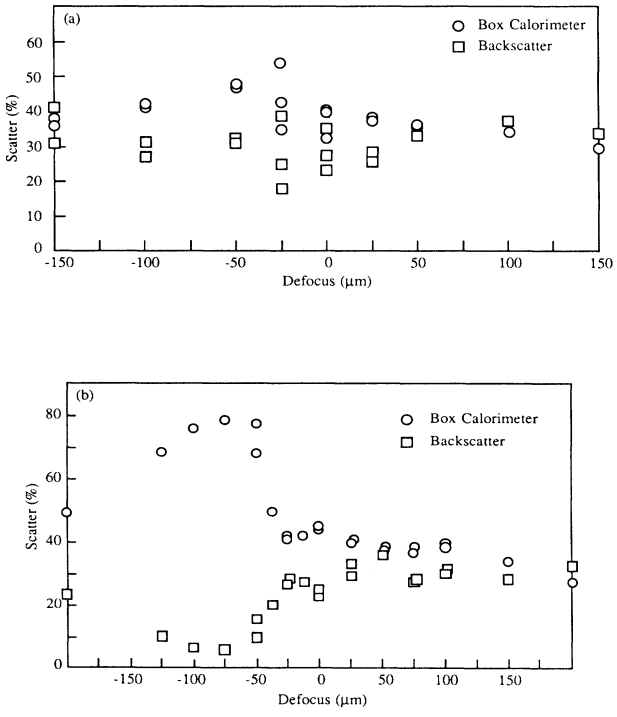

FIG. 3. The fractions of the incident energy scattered into the box calorimeter and back through the $F=1$ lens: (a) 20 psec; (b) 120 psec.

To support the scattered light data some measurements were made angularly resolving the 2ω emission from the plasma. Near -50 μm the 2ω emission spread to larger angles than for the case for $+50$ μm. Very roughly the second harmonic data were consistent with average angles of incidence around 20° for positive defocus and 30°–40° for negative defocus.

To search for the presence of resonance absorption a number of experiments were performed where the average angle of incidence was varied by tilting the targets and absorption measured for p and s polarizations. The results for three different experimental conditions are shown in Fig. 4. Clearly no significant difference in the absorption between the two polarizations was observed and neither was there a detectable resonant rise in absorption with increasing target tilt. A caveat must be appended to these results. The use of the $F=1$ lens system provides a large range of initial angles of incidence at the target surface. As a result the resonance behavior could be smeared out making detection difficult. Furthermore, the strongly focusing beam makes the polarization state at the plasma surface ill defined. We modeled such factors using a simple ray tracing code using a rigid plasma model (see later) and deduced that a significant difference in the absorption for the two polarizations should have been apparent if resonance absorption did, in fact, dominate. Additionally, we replaced the focussing lens by an $F=3$ system to potentially overcome the limitations of the $F=1$ system. Even at the low laser energies used in these experiments, however, no meaningful data could then be obtained since the specularly reflected laser light striking the box calorimeter was sufficiently intense to damage the absorbers and shields changing the sensitivity of the calorimeter from shot to shot.

Information on the energy transfered to the ions was collected by an ion calorimeter and Faraday cup array. In total, nine calorimeters and eight probes were used arranged at angles between 0° and 70° to the target normal in both horizontal and vertical planes. Because angles close to the target normal would normally be obscured by the focusing lens, the targets were tilted to angles of about 35° to obtain a view down the target normal. This situation was not ideal but since the main purpose of these results was to check for serious anomalies in comparison with the box calorimeter the compromise was considered adequate.

The ion calorimeters basically reproduced the absorption behavior for 120-psec pulses shown in Fig. 1(b) although the drop in absorption occurred nearer tight focus. The values of the absorption were consistent with the box calorimeter data for angled targets and a positive to negative defocus asymmetry was obtained with the absorption for -50 μm being only 9% while that at $+50$ μm was 14–15%. A notable features of the results was, however, that the angular distribution of the ion blow off was quite different in the different focal conditions. For negative defocus, both the ion calorimeters and the ion probes showed that most of the energy in the ion distribution was emitted down the target normal. Furthermore, the probes showed that most of the kinetic energy of the ions was contained in the fast ion group. Such data has normally been interpreted as showing that the absorbed energy is transferred to a fast ion blow off because of the generation of fast electrons by resonance absorption. This scenario, if correct, indicates that resonance absorption is strong, even dominant, for negative defocus when the overall absorption is lowest. For positive defocii the fast ions no longer carry most of the absorbed energy. In fact the overall ion velocities drop very significantly and the ion probes reveal an intermediate energy ion group ($\approx$20-keV ions) contributes most of the energy to the ion expansion with that group emerging at angles around 30° to the target normal.

The final experimental data came from the second harmonic calorimetry. These data were obtained considerably later than the rest and 80–100-psec duration pulses were used incident at normal incidence. As a background to this data, we have extensively studied 2ω generation in this laboratory and find no evidence that it is generated by any other process than resonance absorption. We have in our most recent work shown, for example, that the spectrum of the emitted light is fully consistent with resonance absorption in spite of the fact that it is broadened and red-shifted.[11] In older work we show that the angular distribution of the emission can also be fully explained by invoking resonance absorption.[12] As a result, we expect the second harmonic calorimetry to tell us how resonance absorption varies with target position. The data are shown in Fig. 5. What is immediately evident is that the maximum second harmonic occurs close to -30 μm just before the point at which the absorption drops to a minimum. Furthermore, the second harmonic falls to an undetectable level (by the calorimeters) for positive defoci while it remains significant for the equivalent negative positions. We take this data as confirming that the level of resonance absorption is low where the overall absorption peaks and vice versa. This conclusion is the same as that deduced from the ion data.

In summary, therefore, to explain the body of our observations we must search for an absorption mechanism which will produce the high absorption observed at posi-

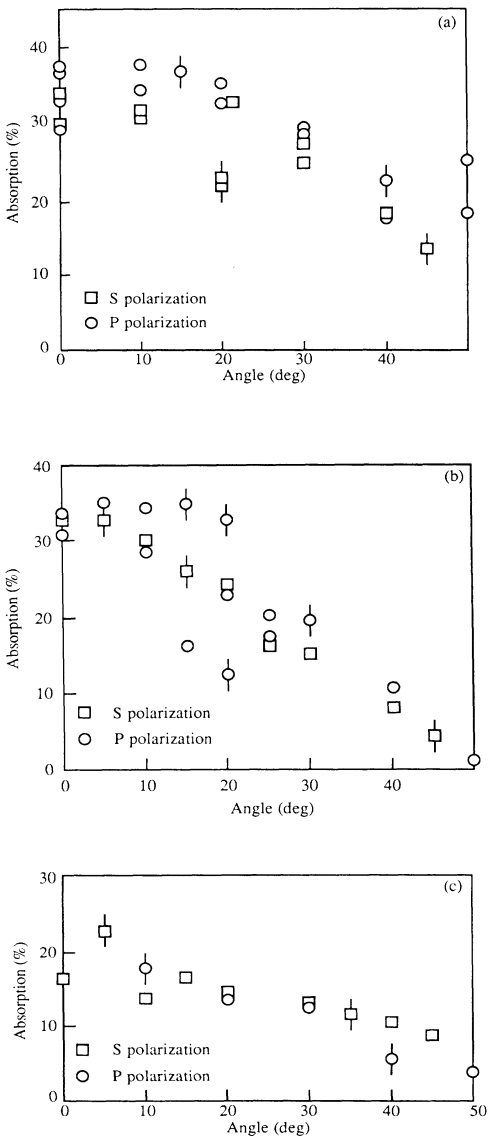

FIG. 4. Absorption as a function of target angle for s and p polarization: (a) 20 psec in focal plane of lens; (b) 120 psec, -12-μm defocus; (c) 120 psec, -75-μm defocus.

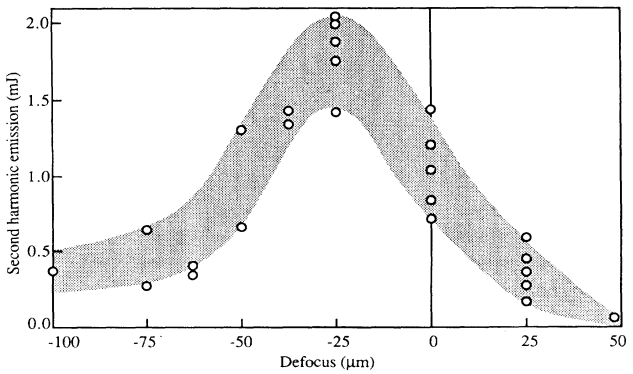

FIG. 5. Total second harmonic emission as a function of target position.

tive defocus but which is switched off for negative defocus by the change in the beam geometry at the target. In what follows we present some simple modelling which we have used to help determine that mechanism.

INTERPRETATION AND MODELING

The experiment described above is a difficult one to model since to do so accurately would require a 3D (three-dimensional) hydrocode, 3D solutions of Maxwells equations (or 2D if we assume cylindrical symmetry), and the inclusion of enough of the physics (profile modification, ion turbulence, stimulated scattering, etc.) which would sensitively affect the absorption to be useful. Code development of this type is well beyond ours as well as most other laboratories' resources. Neither is the problem amenable to an analytic treatment. Hence we are left with the task of developing an approximate model sufficiently robust to allow us to make an "educated" interpretation of these data. Before describing that approach we summarize our knowledge of the plasma.

First, we note that a different behavior is observed for 20 psec in comparison with 120-psec duration pulses. A major difference here is the time for plasma expansion. Short pulses lead to 1D expansion with essentially planar isodensity contours, while for long pulses the expansion becomes two or three dimensional and the isodensity contours would be expected to be convex, as confirmed by interferometry. This should be an essential feature of the model.

Second, we expect the plasma density profile to be characterized by several regions with different density gradients. The laser intensities used here are all high enough for profile modification to occur and hence local steepening should be expected near the critical density surface. Some direct evidence of such steepening has been presented in the literature, although our own interferometric measurements consistently failed to provide information of the critical region actually during the laser pulse. On the other hand the lower densities, particularly below $n_{cr}/4$, have been well characterized and the density scale lengths are typically 5–15 μm—considerably larger than those expected near the critical surface. Plasma profiles have also been predicted from 1D computer codes[13,14] and reproduce these features and their scaling with parameters such as laser intensity. On such bases we can, therefore, make an educated guess of the plasma density profile.

As already mentioned, earlier data on absorption required various anomalous processes to be included before a satisfactory explanation was obtained. In many instances critical surface rippling was used which results in depolarization of the incoming beam and smoothing the angular behavior of resonance absorption. There are a number of analytic approaches that can be used to simulate rippling. It is therefore possible to estimate its effect in a simple model by characterizing the incoming radiation in terms of a modified polarization and angular distribution.[6]

In spite of the relatively high laser intensities, the laser pulse durations are short enough and plasma small enough in extent to assume that many of the scattering instabilities and filamentation or self-focussing would be suppressed. We can, therefore, at least initially neglect them.

On the basis of the previous work, as a starting point we should search for an explanation of our data invoking merely resonance absorption and classical inverse Bremsstrahlung with possibly some influence for critical surface rippling.

It was not possible for us to develop 3D hydrodynamics and hence we chose a simple rigid two dimensional plasma model to simulate the average plasma conditions. In the model the plasma was approximated by a fixed axially symmetric density distribution with predefined density gradients, temperature and shape. To determine the electromagnetic field, a method based on the work of Afanasiev[15] was employed. Using the Wentzel-Kramers-Brillouin (WKB) approximation the rays were traced through the plasma with the level of inverse bremsstrahlung absorption calculated at each point. Once the turning point density was reached a small region of plasma was defined spanning the region from the turning point to a point a few μm beyond the critical density surface. Since the width of this region was small due to strong local density gradients, it could be modelled as a plane plasma slab irradiated with obliquely incident radiation. In this slab absorption due to resonance absorption, inverse Bremsstrahlung and parametric processes could be calculated as could the reflected flux which was then ray traced out of the plasma. Parametric processes could be introduced via an effective collision frequency for those mesh cells where the local intensity exceeded a threshold value. The thresholds used were originally derived for weakly inhomogeneous plasmas and hence some errors could be expected in the steepened region near critical. Ion turbulence could also be included through a density dependent effective collision frequency. Notice that in both these instances localized anomalous absorption processes are introduced through an effective collision frequency. As a result any other physical process that could be characterized in this way could conceivably explain our data. Such an example could be gross critical surface rippling which leads to the formation of cavities and "traps" for the incoming radiation.

The shape of the isodensity contours was modeled by assuming that the laser energy was originally coupled to a region of the target with the same diameter as the beam. The critical surface of the plasma was then allowed to expand at some velocity v_{cr} in three dimensions for the pulse duration τ_p. A spherical plasma shape was then fitted to the axial and radial position of the critical surface. In initial calculations the expansion was assumed to be isotropic, however, in some cases higher axial velocities were used to simulate the jetlike behavior observed in some of our interferometric studies for the underdense region.[16] The critical surface velocity was taken to be the isothermal sound speed c_s with the plasma temperature determined from x-ray measurements.

The density profile was modeled using three exponential density regions; the first in the underdense region with a small density gradient; the second in the critical

region with a much steeper gradient; and the third in the overdense region representing an overdense shelf. The density gradients and transition densities are free parameters in this model and must be chosen with reference to other models and experimental results.

One of the most important parameters was the choice of the density gradient near critical. Some experimental measurements using uv holographic interferometry have been reported[17–20] and these are plotted in Fig. 6. The data at the lower intensities suggest a weak variation of scale length with intensity while Raven and Willi's[20] two high-intensity points indicate a much stronger variation. Various models have provided quite a wide range of results with those of Montes and Willi,[21] for example, showing an increase in scale length with intensity for some ranges and a decrease in others. It is clearly necessary to vary the critical density scale length to assess its affect. Furthermore the data at high intensities do not always agree with indirect measurements such as those reported by Manes *et al.*,[2] where a scale length at 3×10^{16} W/cm^2 of 1.5 μm was deduced.

The transition density (n_1) to the underdense region and that region's scale length were chosen from interferometric data such that $n_1\approx0.3n_{cr}$ and $L_1\approx6$ μm. The upper shelf density n_u has been measured in a number of laboratories and found to have a value almost independent of intensity at $1.2-1.8n_{cr}$.[19] Since it was found that the actual value had little affect on the results n_u was fixed at $1.5n_{cr}$.

An important parameter was the value of the plasma temperature. Again there is some uncertainty and a reasonable choice is important since it affects inverse bremsstrahlung absorption, the thresholds for parametric processes, the plasma expansion velocity, etc. Our own measurements[22] based on x-ray emission suggest that the plasma temperature is approximately constant at about 500 eV throughout the intensity range although this temperature might underestimate the value near the critical density surface where a large population of hot electrons can be expected. This parameter was, therefore, varied to a limited degree to assess its effect.

Calculations were initially made for absorption as a function of defocus assuming that only inverse bremsstrahlung and resonance absorption were operating and using the $I^{-0.49}$ variation for the critical density scale length. Calculations were made for either *p*- or *s*-polarized radiation using the 2D model. The results could be averaged to determine the actual absorption and the difference between the two polarizations also isolated the contribution from resonance absorption.

The first result is shown in Fig. 7 for a 120-psec pulse duration. Notice that here the predicted absorption behaves in almost the opposite way to the experiment. For positive defocus the absorption is low while for negative it is high. Examination of the curves for different polarizations shows that this is due to a very low level of resonance absorption for the positive defocus, where the rays strike the plasma near normal incidence, and a high level for negative defocus where the rays are at oblique incidence. This feature of the result does agree with the experiment with the change of resonance absorption with position closely matching the behavior of the second harmonic conversion shown in Fig. 5.

In the next calculation we turned on anomalous processes by allowing the parametric decay instability to operate near critical or we enhanced the collision frequency near critical to simulate the existence of long-wavelength ion turbulence in the plasma.[23] All other parameters were as before. The results were similar for either the parametric decay or ion turbulence and the latter case with $k\lambda_D\approx0.04$ is shown in Fig. 8. Notice now that the absorption for positive defocus has risen and behaves quite similarly to that observed experimentally. The absorption at negative defocus is slightly lower than the equivalent positive position, although not as large as the difference observed experimentally, and there is a sharp drop in absorption near best focus. This drop in absorption is not observed in the experiments and hence its origin was investigated. It was caused by the $L_c\sim I^{-0.49}$ scaling used in the model which causes a rapid decrease

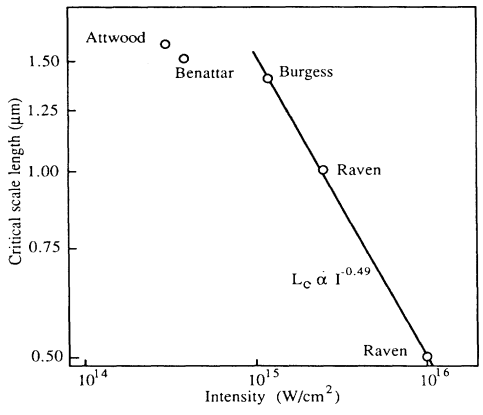

FIG. 6. Experimental measurements of the density scale length in the critical-density region for short pulse 1-μm irradiation. Data are from Attwood *et al.* (Ref. 17), Benattar *et al.* (Ref. 18), Burgess *et al.* (Ref. 19), and Raven and Willi (Ref. 20).

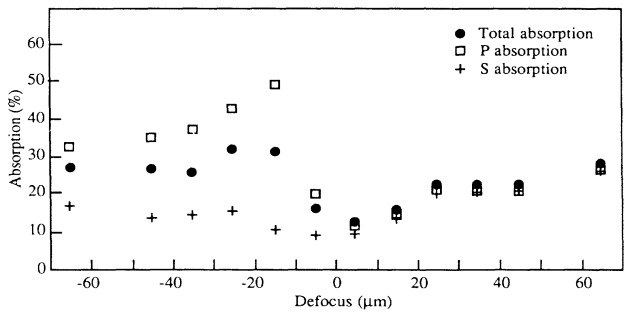

FIG. 7. Results of the calculation of absorption as a function of defocus for a 120-psec pulse assuming that only inverse bremsstrahlung and resonance absorptions are occurring.

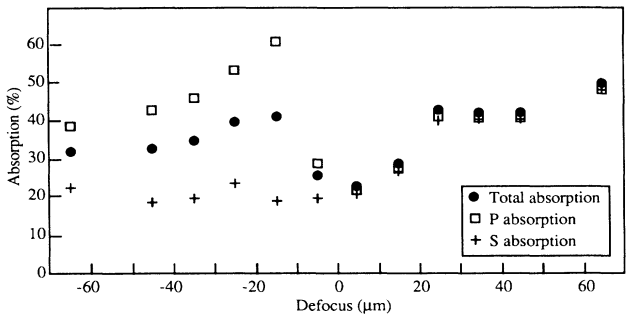

FIG. 8. Absorption as a function of defocus. Conditions as for Fig. 7 but with an enhanced collision frequency operating near critical.

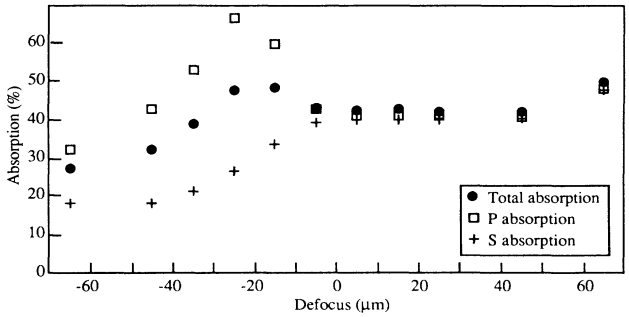

FIG. 10. Results of absorption calculation with the axial plasma expansion velocity increased relative to the radial expansion. Other conditions as for Fig. 9.

in the volume of near-critical-density plasma at the highest intensities which turns off the enhanced absorption. We investigated whether the presence of critical surface rippling or reasonable changes in other plasma parameters could remove this dip and found that it would only disappear if L_c was held approximately constant. Using $L_c \approx \lambda_0$ (λ_0 is the laser wavelength) the result shown in Fig. 9 was obtained. This is much closer qualitatively to the experimental data. Allowing slight asymmetry in the plasma by increasing the axial expansion velocity by about 50% over the radial expansion (to model the observed jet like behavior observed in our interferograms) improved the quantitative agreement with the experiment (Fig. 10).

There are a number of important points about Fig. 10. First, note that a difference still exists between the p and s polarized beams at negative defocus implying that resonance absorption is still turned on, whilst it is not for positive positions. We now find, however, also in agreement with the data, that the total absorption drops just beyond the peak in resonance absorption.

The overall shape of Fig. 10 can be explained as follows. For positive defoci the rays strike the plasma near normal incidence and no resonance absorption occurs. However, the rays then penetrate up to the critical-density surface and the anomalous absorption mechanisms (either the parametric decay or due to long-wavelength ion turbulence, etc.) are effective leading to high absorption. For negative defoci, the rays strike the target at oblique incidence, the conditions for resonance absorption are satisfied, and linear conversion occurs because the evanescent wave can couple from the turning point density ($n_t = n_{cr}\cos^2\theta$, where θ is the angle of incidence) to the critical surface. However, the wave does not directly penetrate the narrow region, whose density is $> n_t$, where the enhanced absorption occurs and, thus, the overall absorption decreases as soon as the peak in resonance absorption has been passed. This picture is quite insensitive to changes in the free variables such as the positions of the density transitions, the exact values of the scale lengths and the plasma temperature. In fact raising the plasma temperature in the critical region to around 1250 eV changes the shape of the curve very little qualitatively but brings the absolute values of absorption closer to the experimental ones. Additionally keeping the features of the model constant but changing the laser pulse duration to 20 psec, thereby making the plasma more one dimensional, results in the predicted absorption behavior shown in Fig. 11 in excellent agreement with the experimental data.

Obviously our model is quite approximate and there are many free variables and omissions. However, we ulti-

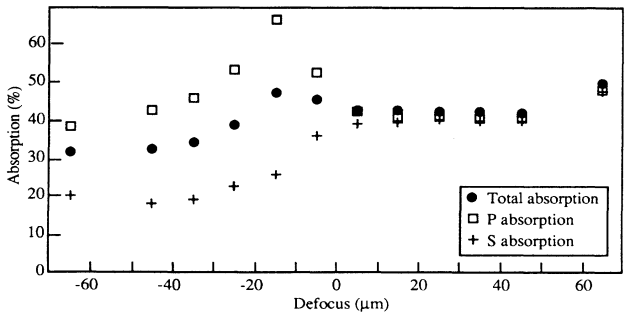

FIG. 9. Absorption as a function of defocus with the critical scale length fixed at λ_0. Other conditions as for Fig. 8.

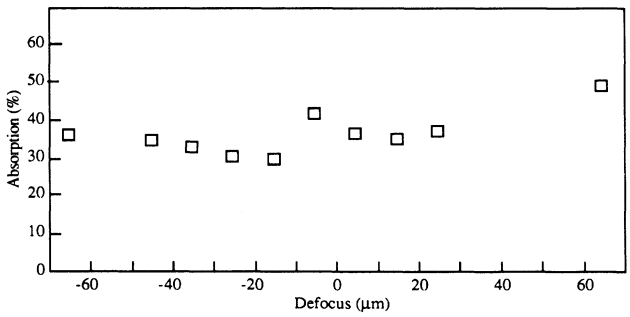

FIG. 11. Absorption for a 20-psec pulse as a function of defocus. The other conditions are similar to those of Fig. 10.

mately obtained good qualitative agreement with our experimental results using a combination of assumptions that can be justified from our and other's experimental data and, furthermore, the basic features of the absorption were quite insensitive to changes in the fine details provided a few key assumptions were included. In no conditions could we find that a combination of resonance absorption and inverse bremsstrahlung alone could explain the data with the absorption being always radically different from the experiment. The assumption that a region of enhanced absorption existed localized near the critical-density surface always produced the right kind of result while still permitting resonance absorption to turn on at negative defocii in agreement with the experiments. Plasma shape was also vital in explaining the results including the differences between the 20- and 120-psec pulse data.

We, therefore, conclude that anomalous absorption involving, for example, either the parametric decay instability or ion turbulence was essential in explaining our data. According to the model near best focus it contributes 60–75 % of the total absorption for rays striking the plasma near normal incidence. For oblique rays, this mechanism essentially turns off and resonance absorption takes over, although the total absorption is always reduced.

The choice of anomalous process between the parametric decay and ion turbulence cannot be determined from these data. If a large contribution from PDI existed, however, we would expect the second harmonic spectra to show evidence of it—our recent work disputes this.[11] The question of whether the threshold for PDI were exceeded would also have to be answered. Furthermore, we have recently gathered a lot of evidence that shows that the critical surface of the plasma is strongly rippled in a manner consistent with the presence of long-wavelength ion waves. As shown by Estabrook[23] such waves give a local enhancement of the collision frequency just near critical, as required. A number of mechanisms can be invoked to generate such waves as the return current driven ion acoustic instability, or turbulence due to stimulated Brillouin scattering, etc. It is perhaps worth noting that in any case the PDI and enhanced collisional absorption involve essentially the same physical process. Both involve decay of the incident electro-magnetic wave into an ion acoustic wave and an electron plasma wave whose energy is subsequently damped by some mechanism. The essential difference between the two reduces to the initial intensity of the ion wave. For PDI it is assumed to be at the noise level while for ion acoustic turbulence the ion wave already exists at high intensity. Obviously the spectrum of the daughter waves can be critically affected by this change in initial conditions in spite of the fact that the same parametric process is involved in both cases. In our opinion our data is more consistent with the operation of the mechanism involving long-wavelength ion acoustic turbulence. A number of factors then fit in place. For example, there appears to be no evidence of a threshold for the absorption process at least over the intensity range that was investigated. The presence of long-wavelength waves near critical fits with the result obtained from the modeling that the effective density scale length near critical seen by the incoming wave was about λ_0 since this also corresponds to the wavelength of the ion fluctuations. Clearly since the local value of the laser wavelength $>\lambda_0$ near the critical surface the wave could not feel a density gradient shorter than that determined by the wavelength of the ion waves. Scattering off these long wavelength ion density fluctuations couples energy to very high phase velocity electron plasma waves that would accelerate some electrons to very high energy. We have observed such high-energy electrons in our studies of electrons transport through layered targets.[24] Overall, therefore, we favor a role for long-wavelength ion acoustic turbulence in explaining these results although we cannot conclusively rule out other processes. More accurate modeling might help resolve some of these issues; however, this is at present outside the scope of our resources.

CONCLUSIONS

A very extensive study of absorption of 20–120-psec duration 1-μm light in laser-produced plasmas at intensities above 10^{14} W/cm^2 has shown that contrary to previous interpretations of absorption data, resonance absorption is not the dominant mechanism. Rather, the light is absorbed in a narrow region close to the critical density surface where an anomalous process such as enhanced collisional absorption due to ion turbulence operates. This conclusion is supported by a large number of measurements involving ion calorimetry, second harmonic calorimety, ion energy analysis, etc. Our previously published work on superthermal electron transport also suggests the number of fast electrons is lower than previously believed,[24] supporting the idea that resonance absorption is not very strong. It is perhaps worth stressing that the actual values of the absorption measured in most conditions are in full agreement with a wide range of data from other laboratories and hence there is no obvious reason why our interpretation should not be equally applicable to previous results.

[1]R. A. Haas, W. C. Mead, W. L. Kruer, D. W. Phillion, H. N. Kornblum, J. D. Lindl, D. MacQuigg, V. C. Rupert, and K. G. Tirsell, Phys. Fluids **20**, 322 (1977).

[2]K. R. Manes, V. C. Rupert, J. M. Auerbach, P. Lee, and J. E. Swain, Phys. Rev. Lett. **39**, 281 (1977).

[3]R. P. Godwin, R. Sachsenamier, and R. Sigel, Phys. Rev. Lett. **39**, 1198 (1977).

[4]M. J. Herbst, J. Grun, J. Gardner, J. A. Stamper, F. C. Young, S. P. Obenschain, E. A. McLean, and B. H. Ripin, Phys. Rev. Lett. **52**, 192 (1984).

[5]D. M. Villeneuve, G. D. Enright, M. C. Richardson, and N. R. Isenor, J. Appl. Phys. **50**, 3921 (1979).

[6]J. J. Thomson, W. L. Kruer, A. B. Langdon, C. E. Max, and W. C. Mead, Phys. Fluids **21**, 707 (1978).

[7]C. Garban-Labauner, E. Fabre, C. Max, F. Amiranoff, R. Fabbro, J. Virmont, and W. C. Mead, Phys. Fluids **28**, 2580 (1985).
[8]W. A. Manheimer and D. G. Colombant, Phys. Fluids **21**, 1818 (1978).
[9]D. R. Bach, D. E. Casperson, D. W. Forslund, S. J. Gitomer, P. D. Goldstone, A. Hauer, J. F. Kephart, J. M. Kindel, R. Kristal, G. A. Kyrala, K. B. Mitchell, D. B. van Hulsteyn, and A. H. Williams, Phys. Rev. Lett. **50**, 2082 (1983).
[10]S. R. Gunn and V. C. Rupert, Rev. Sci. Instrum. **48**, 1375 (1977).
[11]R. Dragila, R. A. M. Maddever, and B. Luther-Davies, Phys. Rev. A **36**, 5292 (1987).
[12]G. B. Gillman, B. Luther-Davies, Opt. Commun. **43**, 194 (1982).
[13]K. Estabrook and W. L. Kruer, Phys. Rev. Lett. **40**, 42 (1978).
[14]F. David, P. Mora, and R. Pellat, Phys. Fluids **26**, 747 (1983).
[15]Yu. V. Afanaseiv, E. G. Gamaliy, N. N. Demchenko, and V. B. Rozanov, Zh. Eksp. Teor. Fiz. **79**, 837 (1980) [Sov. Phys.—JETP **52**, 425 (1980)].
[16]M. D. J. Burgess, B. Luther-Davies, and K. A. Nugent, Phys. Fluids **28**, 2286 (1985).
[17]D. T. Attwood, D. W. Sweeney, J. M. Auerbach, and P. H. Y. Lee, Phys. Rev. Lett. **40**, 184 (1978).
[18]R. Benattar and C. Popovics, Phys. Rev. Lett. **45**, 1109 (1980).
[19]M. D. J. Burgess, R. Dragila, B. Luther-Davies, Opt. Commun. **52**, 189 (1984).
[20]A. Raven and O. Willi, Phys. Rev. Lett. **43**, 278 (1979).
[21]A. Montes and O. Willi, Plasma Phys. **24**, 671 (1982).
[22]M. D. J. Burgess, R. Dragila, B. Luther-Davies, K. A. Nugent, and G. J. Tallents, in *Laser Interaction and Related Plasma Phenomena,* edited by H. Hora and G. H. Miley (Plenum, New York, 1984), Vol. 6.
[23]K. Estabrook, Phys. Rev. Lett. **47**, 1396 (1981).
[24]B. Luther-Davies, A. Perry, and K. A. Nugent, Phys. Rev. A **35**, 4306 (1987).